

# Pressure Drop Analysis in a Pin Type Mini Channel

Nurul Izzati Azmi, Wan Nur Fatini Syahirah Wan Dagang,  
Hazwani Izzati Muhammad Arif, Khairul Imran Sainan\*  
School of Mechanical Engineering, Universiti Teknologi MARA  
\*imransainan@uitm.edu.my

## ABSTRACT

*The mini channel is used widely in industrial applications. The application includes a heat exchanger device, as a part of a cooling system or as a reactant transport channel. However, unlike the pressure drop determination of a piping network, where the loss coefficient values for the bends and fittings are available, similar cannot be done for the mini channel. The loss coefficient values for the channel are rarely determined and reported. The aim of this study is to propose a correlation for the prediction of total pressure drop in a mini channel resulting from the loss coefficient. The results were compared against a numerical simulation. A 42 mm x 50 mm pin type mini channel was used as the sample of the study. The fluid was hydrogen. The flow regime was kept as laminar. The numerical simulation was performed on the whole active area. The correlation was calculated using the loss coefficient values of bends that were determined beforehand. Three correlations were proposed. Statistical values were used as the comparison parameters. Based on the results, an almost similar pressure drop was predicted by correlation III (diff. mean  $\pm$  SD = 0.005  $\pm$  0.006 kPa). The correlation I and correlation II were not able to predict the expected results at all. The results were from a low Reynolds (range of Re < 200) number. In general, the correlation proposed successfully predicted the pressure drop in a pin-type mini channel using the loss coefficient value of the individual bends.*

**Keywords:** Mini channel; Pin type; Pressure drop; Loss coefficient value

## Introduction

In recent years, small channels are used widely in the industry such as in electronics [1][2], fuel cells [3][4], and electric vehicle batteries [5][6]. The

usage includes as a heat transfer device, reactant transport channel, or as a part of a cooling system. A mini channel is a channel with a very small diameter. An existing paper in [7][8] proposed the classification of these types of channels. The channel was classified into mini ( $200 \mu\text{m} \geq D_h > 3000 \mu\text{m}$ ) channel based on the hydraulic diameter size,  $D_h$ .

In most cases, there are two factors affecting the value of pressure drop in a mini channel. The friction factor and the loss coefficient value. The friction factor is influenced by material roughness. This restricts the fluid from flowing. The loss coefficient,  $k$  is caused by the bends, fittings, and the change of dimension within the system. A study by [9], concluded that at low Reynold's number, the mini channel has a similar friction factor with the conventional theory. Studies by [10][11] stated that friction factor was dependent on the channel aspect ratio. The long-wetted channel perimeter and small  $D_h$  usually have a high-pressure drop. In addition, a proper evaluation  $D_h$  is important to ensure a valid friction factor value. Paper by [12], pointed out that friction factor is strongly related towards the  $D_h$ . Meanwhile, the loss coefficient,  $k$  is influenced by the geometrical parameter. The abrupt change of flow contributed to the pressure drop. This is true for the circular piping network. However, the contribution of these losses on the mini channel is rarely determined and emphasized. Most of the studies were focused on the total pressure drop.

Determination of pressure drop for a mini channel is not an easy task. In a normal case, complete experimentation or simulation needs to be conducted. In contrast, a pump engineer, for example, is able to estimate the pressure drop of a circular piping network using Bernoulli's equation. Apart from the friction factor, the loss coefficient,  $k$  was also tabulated. The tables are widely available [13][14]. The values were extensively determined [15][16]. However, a similar estimation cannot be done for the mini channel. The loss coefficient,  $k$  is rarely determined and reported. In addition, limited study has determined or proved that the pressure drop of a mini channel is able to be estimated using such a method.

In this study, the authors are trying to fill the gap stated above. A pin-type flow channel was used as the sample of the study. The results from a numerical analysis were compared with the conventional calculation method. Initially, the loss coefficient values of each bend were determined. Three correlations were proposed.

## Methodology

### Test sample

A pin-type flow channel was used as the test sample. The test sample selected was based on an industrial fuel cell. A pin-type flow channel has a network of series and parallel flow paths. The active area is 42 mm x 50 mm. The channel

width and height are 2 mm x 2 mm respectively. There are a total of 110 pins with a dimension of 2 mm x 2 mm each. Figure 1 shows the schematic diagram of the pin-type mini channel used. As seen, the channel has a combination of square pins and bends sections.

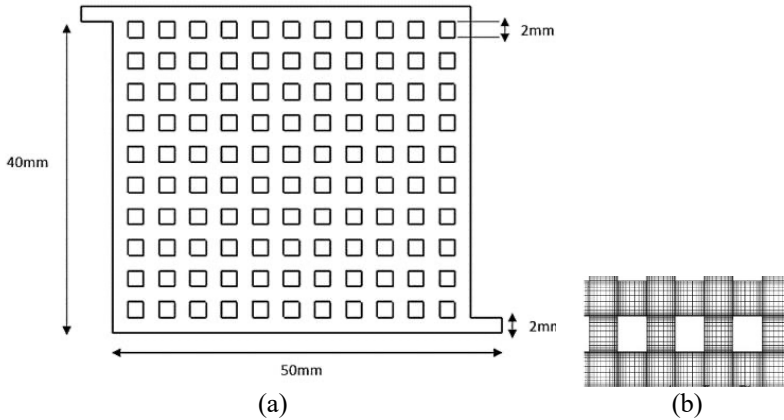


Figure 1: A pin type mini channel where (a) the test sample and (b) the structured grid setup used.

### Physical properties and operating parameters

The fluid analyzed was hydrogen. The temperature was assumed at 20 °C. Table 1 shows the physical properties and the operating parameters used. Based on the fluid temperature, the density and the dynamic viscosity were 0.084 kg/m<sup>3</sup> and 8.805 x 10<sup>-6</sup> kg/m.s. The flow was kept laminar. The operating pressure was set as atmospheric.

Table 1: Physical properties and operating parameters

Parameter	Value	Unit
Operating pressure, P	101325	Pa
Density, $\rho$	0.084382	kg.m <sup>-3</sup>
Dynamic viscosity, $\mu$	8.8054 x 10 <sup>-6</sup>	kg/m.s
Reynolds number, Re	Laminar	-
Operating temperature, T	20	°C
Cell active area, A	40x50	mm <sup>2</sup>

\*The wall was assumed to be smooth. The calculations carried out under the pressure-velocity coupling

### Numerical solution

A numerical simulation was carried out on the test sample. A structured grid setup was used. Prior to the simulation, a grid independence study was performed. At least 10 grids per minimum length with a growth rate of 1.2 were applied. The number of grids was increased accordingly to eliminate the effect of geometry discretization. The outlet velocity was observed for consistency. This is vital to ensure the accuracy of results. Proper boundary conditions were set. The model chosen was based on the standard laminar flow. The inlet boundary was set based on the Reynolds ( $2 < Re < 1000$ ) number. Analyses were ended if the loss coefficient values were becoming constant. Velocity inlet was set at the inlet boundary. At the outlet, the pressure was kept atmospheric. This is similar to the setup by [16] where uniform velocity distribution was prescribed at the inlet and average static pressure at the outlet. In contrast with the study by [5], the heat transfer was neglected, therefore, the energy equation was not considered. SIMPLE algorithm was used [17]. The governing equations are mass conservation and the conservation of momentum. The equations are as the following:

Mass conservation equation:

$$\frac{\partial(U_i)}{\partial x_i} = 0 \quad (1)$$

Momentum conservation equation:

$$\frac{\partial(U_j U_i)}{\partial x_i} = -\frac{1}{\rho} \frac{\partial P}{\partial x_i} + \frac{\partial}{\partial x_i} \left[ \nu \frac{\partial U_i}{\partial x_j} \right] \quad (2)$$

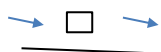
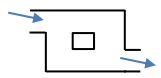
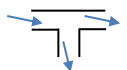
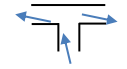
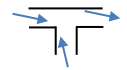

where  $i = 1, 2, 3$  etc. In this case,  $U_i$  is the component of velocity in the  $i$ -direction,  $P$  is the static pressure,  $\rho$  and  $\nu$  are the fluid density and kinematics viscosity, respectively. The model constants were not altered, and the default standards were used. The wall was assumed to be smooth. A no-slip condition was applied to the wall boundaries. The calculations were carried out under the velocity-pressure coupling. The total pressure of the inlet and the outlet were the main parameters observed.

### Computation of proposed correlations

Three correlations were proposed. The correlation I, correlation II, and correlation III. Table 2 shows the individual bends that were involved with the computation. The correlation I assumed the loss coefficient was based on a square pin in a straight channel. The total value was determined by multiplying the  $k$  value by the number of pins. Correlation II assumed the loss coefficient was based on a square pin in a  $z$  channel. The value was also a sum of the number of pins. Correlation III was based on the individual bends within the pin-type channel. A total of 19 tee branch ends, 110 tee branch entrances, 2 of

the 90° sharp edges, and 1 tee branch exit bends were considered. Subsequently, the pressure drop was calculated using Bernoulli's equation. The comparison of these values against the simulation is shown in Table 3.

Table 2: The individual bends that were estimated

Bends	Geometry
Pin in straight channel	$k_a$ 
Pin in z-geometry	$k_b$ 
Tee branch entrance	$k_c$ 
Tee branch end	$k_d$ 
Tee branch exit	$k_e$ 
90° sharp edge	$k_f$ 

The total loss coefficient,  $k_T$  of each correlation was calculated. The equation is used as the following:

The correlation I equation:

$$\sum k_T = 110k_a \tag{3}$$

Correlation II equation:

$$\sum k_T = 110k_b \tag{4}$$

Correlation III equation:

$$\sum k_T = 19k_d + 110k_c + 2k_f + k_e \tag{5}$$

Therefore, the losses were estimated by:

$$h_L = \frac{\sum k_T v^2}{2g} \tag{6}$$

where the  $v$  is the average velocity within the channel.

## Results

### Validation

Validation was performed against an existing work [18]. Figure 2 shows the results from the comparison. The geometry used was a 90° sharp edge bend channel with a rectangular hydraulic diameter. The hydraulic diameter,  $D_h$  was 1 mm. A similar trend was observed in the present work. The loss coefficient,  $k$  decreased with the increase of Reynolds number. The error was reduced at a larger Reynold’s number. Both results were in good agreement.

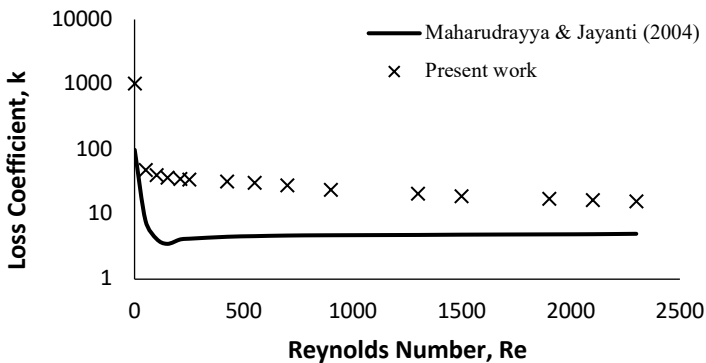


Figure 2: Comparison between the present and the existing work.

### Loss coefficient, $k$ for the individual bends

The numerical simulation on the individual bends produced a series of loss coefficients,  $k$  values. The values are varied based on the Reynolds number. The values were found by comparing the results from two corresponding channels. As an example, take the pin in  $z$ . Two channels were analyzed, a pin in a  $z$  channel and a  $z$  channel without the pin. Theoretically, the smaller pressure drop is expected by the  $z$  channel. This is because of the absence of the pin. Meanwhile, the larger pressure drop is expected by the pin in the  $z$  channel. Subtracting between both values, produced the net loss coefficient values,  $k$  for the pin. The calculation was continued at different Reynolds numbers. A similar approach was performed to find the loss coefficients at

different geometry. Subsequently, the pressure drop of the proposed correlations was determined. In order to achieve this, the information from the tabulated data was referred to. Interpolation should be used when necessary.

**Results of the proposed correlations against the simulation data**

The results from the proposed correlations were compared against the simulation data. The three correlations together with the simulation data recorded similar friction factors. Similar to the study by [19], the trend decreased with the increase of Reynolds number. As mentioned, the channels were assumed to be smooth. The effect of surface roughness was not considered. In contrast with the research by [20], the friction factor was solely contributed by the channel cross-sectional area. This was intentional to eliminate the effect of the major loss. As the major loss is constant, the effect of the loss coefficient can be observed. In addition, horizontal orientation was assumed. The previous study by [21], shows that a channel with a vertical orientation contributed towards the sum of pressure drop.

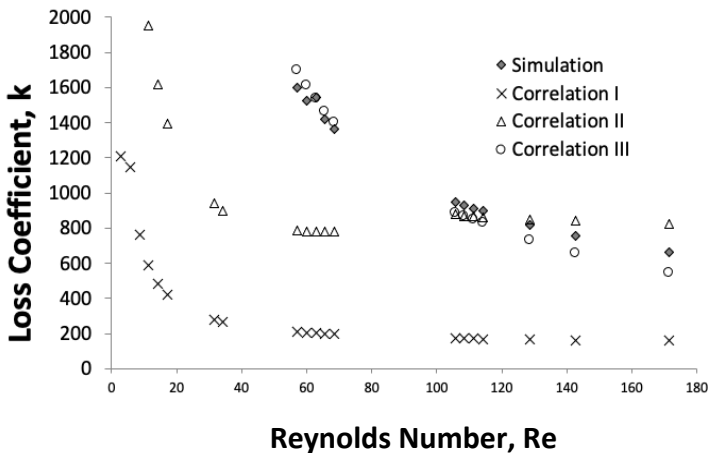


Figure 3: Loss coefficient values for Correlation I, II and III.

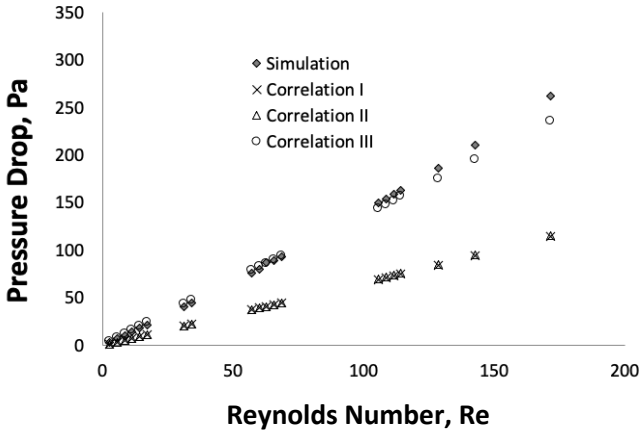


Figure 4: Pressure drop for Correlation I, II and III.

Figure 3 shows the comparison of the loss coefficient. The values of all three correlations decreased with the increase of Reynold’s number. Simulation data recorded a similar trend. Almost similar loss coefficient values were predicted by correlation III. The correlation I and correlation II were not able to predict the loss coefficient result at all. Figure 4 shows the comparison of the pressure drop. A descriptive statistical analysis was performed as shown in Table 3. The pressure drops of correlation I (mean  $\pm$  SD = 0.044  $\pm$  0.034 kPa), correlation II (mean  $\pm$  SD = 0.043  $\pm$  0.034 kPa) and correlation III (mean  $\pm$  SD = 0.091  $\pm$  0.070 kPa) increased with the increase of Reynolds number. Simulation (mean  $\pm$  SD = 0.094  $\pm$  0.077 kPa) data recorded a similar trend. As expected from the results of the loss coefficient, only correlation III (diff. mean  $\pm$  SD = 0.005  $\pm$  0.006 kPa) successfully predicted the pressure drop.

Table 3: Descriptive difference of the proposed correlations

Rater	Difference mean $\pm$ SD	% mean difference	SD as CV%
Correlation I	0.050 $\pm$ 0.042	53.5	45.7
Correlation II	0.049 $\pm$ 0.042	53.1	45.3
Correlation III	0.005 $\pm$ 0.006	5.41	6.63

Correlation I (diff. mean  $\pm$  SD = 0.050  $\pm$  0.042 kPa) and correlation II (diff. mean  $\pm$  SD = 0.049  $\pm$  0.042 kPa) failed to do the same. Contrary to the other two correlations, Correlation III considers all bends. Thus, it produced better predictions.



## Conclusion

The aim was satisfied and achieved. A correlation was proposed. Correlation III produced almost similar results with the pin-type channel. The tabulated data from each bend and fittings were valid. The authors successfully proved that the mini channel can be estimated conventionally.

## Acknowledgment

The authors would like to thank Fakultas Kejuruteraan Mekanikal, RMI UiTM through the MOHE grants (600-RMI/FRGS5/3(54/2012) and (600-RMI/ERGS 5/3 (17/2013) for providing the facilities and the financial support.

## References

- [1] S. M. Sohel Murshed and C. A. Nieto de Castro, "A critical review of traditional and emerging techniques and fluids for electronics cooling," *Renewable and Sustainable Energy Reviews*, vol. 78. Elsevier Ltd, pp. 821–833, Oct. 01, 2017.
- [2] M. Bahiraei and S. Heshmatian, "Electronics cooling with nanofluids: A critical review," *Energy Conversion and Management*, vol. 172, pp. 438–456, Sep. 15, 2018.
- [3] J. Wu, Y. Li, and Y. Wang, "Three-dimension simulation of two-phase flows in a thin gas flow channel of PEM fuel cell using a volume of fluid method," *Int. J. Hydrogen Energy*, vol. 45, no. 54, pp. 29730–29737, Nov. 2020.
- [4] K. Imran Sainan, A. S. Tijani, I. A. Zakaria and W. A. N, W. Mohamed, "Study of multiple 2:1 and single 1:1 inlet/outlet ratio for serpentine PEMFC performance," *J. Mech. Eng.*, vol. 5, no. 6, pp. 1–9, 2018.
- [5] Y. Kim, M. Kim, C. Ahn, H. U. Kim, S. W. Kang, and T. Kim, "Numerical study on heat transfer and pressure drop in laminar-flow multistage mini-channel heat sink," *Int. J. Heat Mass Transf.*, vol. 108, pp. 1197–1206, May 2017.
- [6] K. Monika, C. Chakraborty, S. Roy, S. Dinda, S. A. Singh, and S. P. Datta, "Parametric investigation to optimize the thermal management of pouch type lithium-ion batteries with mini-channel cold plates," *Int. J. Heat Mass Transf.*, vol. 164, p. 120568, Jan. 2021.
- [7] S. G. Kandlikar and W. J. Grande, "Evolution of microchannel flow passages-thermohydraulic performance and fabrication technology," *Heat Transf. Eng.*, vol. 24, no. 1, pp. 3–17, 2003.
- [8] S. G. Kandlikar, "Fundamental issues related to flow boiling in minichannels and microchannels," *Exp. Therm. Fluid Sci.*, vol. 26, no. 2–

- 4, pp. 389–407, Jun. 2002.
- [9] M. Mala and D. Li, “Flow characteristics of water in microtubes,” *Int. J. Heat Fluid Flow*, vol. 20, no. November 1997, pp. 142–148, 1999.
- [10] X. F. Peng and G. P. Peterson, “Convective heat transfer and flow friction for water flow in microchannel structures,” *Int. J. Heat Mass Transf.*, vol. 39, no. 12, pp. 2599–2608, 1996.
- [11] H. Wang, Z. Chen, and J. Gao, “Influence of geometric parameters on flow and heat transfer performance of micro-channel heat sinks,” *Appl. Therm. Eng.*, vol. 107, pp. 870–879, Aug. 2016.
- [12] N. Caney, P. Marty, and J. Bigot, “Friction losses and heat transfer of single-phase flow in a mini-channel,” *Appl. Therm. Eng.*, vol. 27, no. 10, pp. 1715–1721, Jul. 2007..
- [13] Y. A. Cengel and J. M. Cimbala, *Fluid Mechanics - Fundamentals and Applications*, 3rd Edition. New York: Mc Graw Hill Education, 2014.
- [14] B. R. Munson, T. H. Okiishi, W. W. Huebsch, and A. P. Rothmayer, *Fundamentals of Fluid Mechanics*, 7th Edition. Hoboken, NJ: John Wiley & Sons, 2013.
- [15] M. S. de Moraes *et al.*, “Experimental quantification of the head loss coefficient K for fittings and semi-industrial pipe cross section solid concentration profile in pneumatic conveying of polypropylene pellets in dilute phase,” *Powder Technol.*, vol. 310, pp. 250–263, Apr. 2017.
- [16] P. Csizmadia and C. Hos, “CFD-based estimation and experiments on the loss coefficient for Bingham and power-law fluids through diffusers and elbows,” *Comput. Fluids*, vol. 99, pp. 116–123, 2014.
- [17] S. V. Patankar, *Numerical Heat Transfer and Fluid Flow.*, 1st Edition. United States: Taylor & Francis, 1980.
- [18] S. Maharudrayya, S. Jayanti, and A. P. Deshpande, “Pressure losses in laminar flow through serpentine channels in fuel cell stacks,” *J. Power Sources*, vol. 138, no. 1–2, pp. 1–13, Nov. 2004.
- [19] H. Zhao, Z. Liu, C. Zhang, N. Guan, and H. Zhao, “Pressure drop and friction factor of a rectangular channel with staggered mini pin fins of different shapes,” *Exp. Therm. Fluid Sci.*, vol. 71, pp. 57–69, Feb. 2016.
- [20] B. Dai, M. Li, and Y. Ma, “Effect of surface roughness on liquid friction and transition characteristics in micro- and mini-channels,” *Appl. Therm. Eng.*, vol. 67, no. 1–2, pp. 283–293, Jun. 2014.
- [21] M. Ashrafi and M. Shams, “The effects of flow-field orientation on water management in PEM fuel cells with serpentine channels,” *Appl. Energy*, vol. 208, no. 17, pp. 1083–1096, 2017.